e-Polymers **2008**, no. 113

http://www.e-polymers.org

ISSN 1618-7229

Influence of annealing on microstructure & molecular orientation, thermal behaviour, mechanical properties and their correlations of uniaxially drawn iPP thin film

Sayant Saengsuwan [*]

[*]Department of Chemistry, Faculty of Science, Ubon Ratchathani University, Varin Chamrap, Ubon Ratchathani 34190, Thailand; fax: +66 45 288379; e-mail: sayant@sci.ubu.ac.th

(Received: 11 January, 2008; published: 27 August, 2008)

Abstract: The influence of annealing on the microstructure and molecular orientation, thermal behaviour and mechanical properties of uniaxially drawn iPP thin film was studied by wide-angle X-ray diffraction, differential scanning calorimetry and tensile testing, respectively. The correlations of mechanical and microstructural properties of annealed films were also examined. The transformation of smectic phase of iPP to the α-form was more pronounced with increasing annealing time and temperature. The true and apparent crystallinities and crystal thickness were strongly enhanced with annealing time and temperature. The relative molecular orientation tended to increase with annealing time. These results caused the significant improvement of modulus and tensile strength of the annealed films in both machine (MD) and transverse (TD) directions. The increases in MD-Young's modulus and MD-tensile strength were well correlated with the increase in true crystallinity obtained in equatorial scans. Some relationship between the increase in crystal thickness and the increase in Young's modulus in both MD and TD directions was also found.

Introduction

Polypropylene (PP) is one of the largest volume polyolefin in the industry of plastics due to its wide range of physical properties, relative ease of processing, recyclability and low cost, compared to other engineering thermoplastics. It is widely used in many different applications such as for appliances, packaging, textiles, reinforcing fibers, monofilaments, film, automotive parts, reusable containers of various types, and other durable items for home and garden uses. Additionally, the ranges of properties and applications for PP may extend in various ways by physical treatments, for example, thermal treatment [1-3] and plastic deformation [4, 5]. PP can be also modified by adding fillers and/or blended with other polymers [6-7] and recently was used as a matrix polymer to blend with nanoparticles/carbon nanotubes to form nanocomposite materials [8, 9], in which the main field of attention is the enhancement of mechanical properties.

Particularly, the polymorphism of isotactic PP (iPP) has been attracting attention of both polymer physics and technology. When crystallized from the molten state, iPP chains adopt a 3/1 helix, indicating that it takes three monomer units to make one helical turn. The iPP often presents three different crystalline forms, namely, the monoclinic α-modification, trigonal β-modification, and triclinic γ-modification, depending on the crystallization conditions [10-17]. Among these polymorphs, the α-form is the thermodynamically stable crystalline modification and is predominate

under the usual crystallization conditions. The α species are characterized by the presence of transverse crystallites in addition to the main structure of radial lamellae, the so-called “cross-hatching” morphology. Also, the wide angle X-ray diffraction (WAXD) patterns of α-form show the characteristic peaks at 2θ about 14.1 (110), 17.0 (040), 18.5 (130), 21.3 (111) and 21.8° (041) [3, 5, 11, 12, 18]. The β-form is less prevalent because of its lower stability than α-form and results from crystallization under a temperature gradient, under shear during processing or in the presence of specific nucleating agent [13-15]. Finally, the γ-form is the rarest and can be observed only sporadically, especially, only when low molecular weight iPP crystallizes under high pressure [16, 17].

Furthermore, there is also an intermediate crystalline order of iPP, which can be obtained by rapid quenching of the molten isotactic iPP to room temperature. This intermediate state is between ordered and amorphous phases, and widely known by various names such as “quenched” [19], “mesomorphic” [20,21], “paracrystalline” [22], nano-crystallites [23], condis crystal [24] and a well known “smectic” phase [25-27]. Later, it was also found that the smectic phase could be obtained by cold drawing of iPP film at room temperature [28-30]. However, the full evidence for the smectic phase in iPP has not been documented. The description of the smectic phase can be quite confusing in the literature. Natta and Coradini [26], who first observed this phase in 1960, pointed out that this phase is characterized by parallel helices having disorder in the lateral packing, but maintaining some degree of positional correlation along the chain axis between adjacent helices. After that, Miller [22] suggested that the structure of the quenched phase displayed two broad and diffuse X-ray diffraction profiles, located at 2θ angles of 14.8 and 21.2°, which were amorphous and paracrystalline phases. The location of the former peak is close to that of the diffuse amorphous peak from the iPP melt, but the latter peak indicates a higher order of the structure from the helical chains. McAllister *et al.* [31] showed that 60% of the material in the smectic form of PP was amorphous, remaining in microcrystalline arrays of cubic or tetragonal symmetry and they also estimated the crystallite size of smectic form to be about 3 nm which was smaller than that of α-phase (3-5 nm) and β-phase (5-10 nm) [32-34]. Boder *et al.* [32] used X-ray evidence to indicate that the structure composed of microcrystallites of monoclinic habit. According to Saraf and Porter [35], they reported that the smectic phase was formed by 3/1 helices highly oriented, but the lateral packing of such helices was highly disordered.

Although the smectic phase of iPP is relatively stable at room temperature for long period of time, it can be transformed into the monoclinic iPP phase (α-iPP), the most stable phase, on heat treatment at temperature above 70 - 80 °C [20,36,37], or by applying of plastic deformation to the materials [5]. Thus, the annealing on iPP causes a decrease in the amount of both amorphous and smectic phases while the amount of monoclinic phase, the crystal size, and the degree of perfection are increased and leads to a significant improvement in the mechanical properties of the samples [1-3, 20, 21, 38-41]. The transformation of the smectic phase to the monoclinic phase can be detected by different experimental techniques such as WAXD, density and differential scanning calorimetry (DSC) [1-3, 41]. In addition, it is well known that annealing of polymer materials after fabrication makes the properties of sample to change at microscopic level in different phenomena, such as reorganization of amorphous segment through chain mobility, rearrangement of crystal segments and reduction/elimination of defects and residual stress and strain

[42]. Such annealing also changes the morphological modification of crystal regions through lamellae thickening in the semi-crystalline polymers. The effect of annealing at macroscopic level is one of important factors to improve mechanical properties of the materials such as Young's modulus, impact strength, tensile strength, and toughness [1-4, 38-41]. From above reasons, the effects of annealing of PP on its mechanical, impact and fracture properties, crystalline structure, phase transformation, crystallization behavior, elastic response as well as morphology have gained much attention in the last decade [1-3, 39, 40, 43-47].

Poussin *et al.*, 1998, investigated the influence of thermal treatment on the structure of iPP sheet (5 mm thick), reported that crystallinity, density and apparent crystal size of the α-phase were rapidly increased in the first five minutes of treatment at 125 °C [2]. They also claimed that a temperature of 125 °C favours molecular mobility in the amorphous phases, and the motion of the chains led to a more stable thermodynamic position. Ferrer-Balas *et al.*, 2001, evaluated the influence of the annealing on the properties of iPP film (95 μm thick) at the temperature range of 80 - 150 °C, showed that the smectic phase of quench iPP film transforms gradually into α-phase as the annealing temperature is increased [3]. Moreover, the tensile properties of such annealed iPP films were highly improved due to the microstructural changes. The improvement of tensile properties was very well correlated to the crystallinity, crystal size and smectic phase melting temperature. Later, Pegoretti *et al.*, 2003, however, showed that annealing sample of iPP at 75 °C for 45 days did not markedly affect the tensile modulus, yield stress and stress at break of pure PP and the blend [44]. In addition, Drozdov *et al.*, 2003, also concluded that annealing in the low-temperature ranges (110-130 °C) did not affect the material constant that reflected the elastoplastic response of iPP but increased in brittleness of secondary lamellae developed at higher temperature [45]. Recently, Zia *et al.*, 2006, studied the mesomorphic nanocrystals in iPP films revealing that annealing at temperature within the melting range of iPP allowed the formation of lamellae by coalescence of nodules, evidenced by a distinct blocky structure of lamellae [46]. Jia and Raabe, 2006, also presented that the heat treatment after rolling iPP sheets led to the recrystallization of amorphous material and to a strong enhancement of the fiber orientation component, which is explained in terms of an oriented nucleation mechanism where amorphous material aligns along existing crystalline lamellae blocks which prevailed during the preceding deformation [39]. Song and co-worker, 2006, concluded that the annealing conditions had the important influence on the molecular orientation and deformation behavior of annealed iPP thin films [47].

In the present work, the influence of annealing conditions, in the low-temperature ranges (at 110 and 130 °C), on microstructural transformation, molecular orientation, thermal behaviour and mechanical properties of the uniaxially drawn iPP thin films (~20 μm thick) is examined. It is also interesting to study the correlations of the true crystallinity calculated from WAXD patterns in both equatorial and meridional sections with their respective mechanical properties in machine (MD) and transverse (TD) directions, respectively.

Results and discussion

Microstructural development

The Wide angle X-ray diffraction (WAXD) patterns of the uniaxially drawn iPP films annealing at 110 and 130 °C at different times are presented in Figs. 1 and 2,

respectively. It can be seen that the WAXD patterns of unannealed drawn iPP film (UA) in both equatorial (EQ) and meridional (ME) scans consist of two intense broad peaks at 2θ equal 15.4 and 21.4°, and a shoulder peak at 28.8°. This pattern has been well known as the 'smectic phase' of iPP as first observed by Natta and Coradini [26] and by the latter researchers [27-38]. In general, the smectic phase of iPP can transform to the more stable crystalline phase (α-form) through annealing at appropriate temperature, i.e. 70-150 °C or by applying plastic deformation [3,5,20,36-41]. Such results have also confirmed in our previous work for iPP thin film annealed at 110 °C for 2 h [48]. In the present work, the WAXD patterns of iPP films annealed at 110 and 130 °C at different times have again confirmed the transformation of smectic phase PP to the α-form as shown in Figs. 1 and 2, respectively.

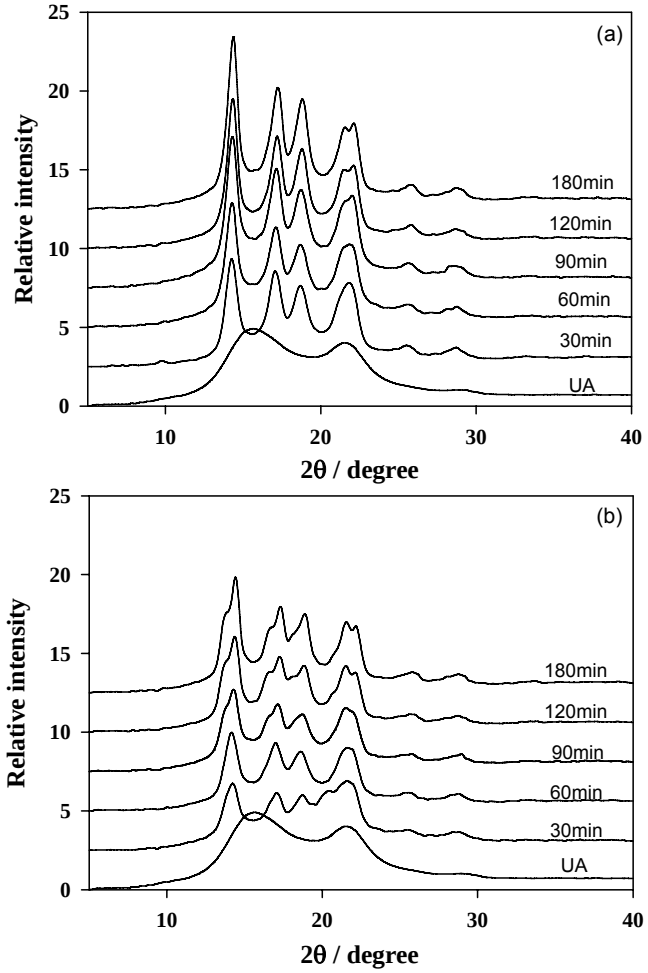

Fig. 1. WAXD patterns of the uniaxially drawn iPP thin films annealed at 110 °C at various times in (a) equatorial (EQ) and (b) meridional (ME) scans.

The WAXD patterns of annealed iPP films in both EQ and ME scans represent the characteristic peaks of the well-known α-form (monoclinic phase) at 2θ ≈ 14.3 (110), 17.2 (040), 18.8 (130), 21.4 (111) and 21.8° (041) [3, 5, 25, 26]. It is clearly seen that the WAXD patterns obtained from the ME scans are not much sharp and well-defined as those measured in the EQ scans. As the annealing time and temperature increase, the WAXD intensity profiles of the samples in both sections are sharper and more intense. This suggests that the transformation of smectic phase to

monoclinic phase is more pronounced with increasing annealing time and temperature, corresponding to the longer time for rearrangement and the higher thermodynamic molecular motion ability of iPP molecular chain, respectively.

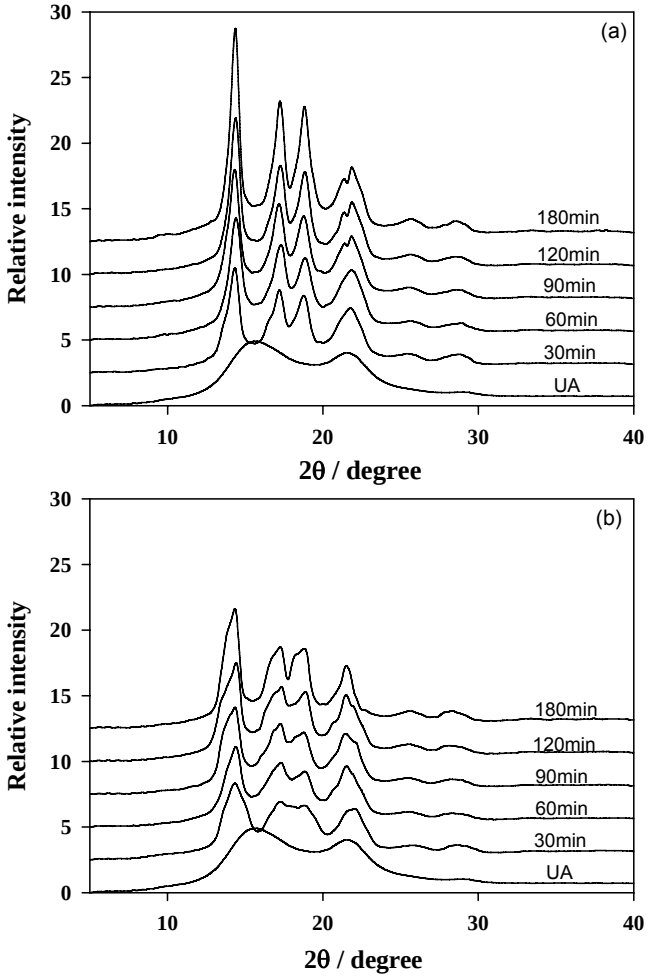

Fig. 2. WAXD patterns of the uniaxially drawn iPP thin films annealed at 130 °C at various times (a) equatorial (EQ) and (b) meridional (ME) scans.

In addition, the true crystallinity (X_c) and the apparent crystal thickness (L) of the annealed samples evaluated from WAXD patterns are shown in Fig. 3a and 3b, respectively. It is seen that the X_c and L strongly increase in the first 60 min of annealing at both annealing temperatures; after that it tends to be unchanged. It is also found that X_c of the films annealed at 130 °C is higher than that of films annealed at 110 °C at the same annealing time, which is similar to the results obtained from DSC. Also, the calculated L of iPP films annealed at 130 °C is thicker than that of films annealed at 110 °C at the same conditions. These results indicate that the crystalline phase of α-form has higher degree of perfection and thicker crystal size with increasing annealing time and temperature which agrees well with the increasing of T_m^{sm} and degree of crystallinity measured by DSC (see Fig. 5 and 6, respectively). Furthermore, it should be noted that the rate of crystallization for the

films annealed at 130 °C is found to be higher than that of the films annealed at 110 °C, owning to the higher thermodynamic mobility of molecular chain [3].

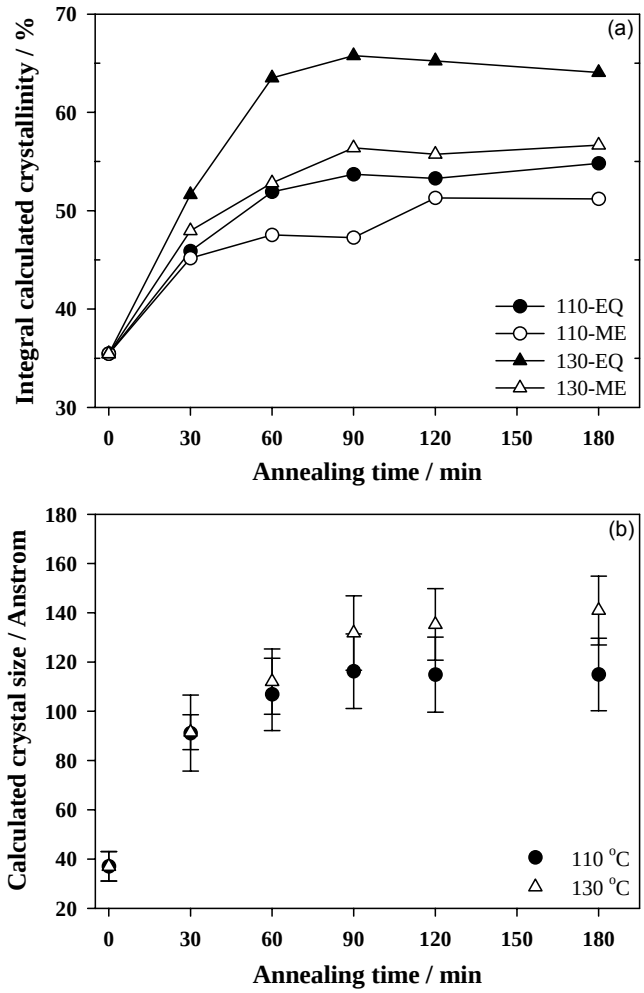

Fig. 3. Plot of (a) true crystallinity in both EQ and ME sections and (b) the apparent crystal size as a function of annealing times for the uniaxially drawn iPP films annealed at 110 and 130 °C.

In order to roughly qualify the molecular orientation of annealed drawn iPP films, the comparison between the maximum peak intensity of (110) peak of EQ and ME scans is considered to estimate the relative level of preferred orientation. The previous studies have also shown that the uniaxially drawn iPP thin film annealed at 110 °C for 2 h exhibited slight anisotropy indicating that there was some small difference in the peak intensity in azimuthal scans [48]. Therefore, by comparison of the difference in the peak intensity of (110) in equatorial (azimuthal angle = 90°) and meridional scans (azimuthal angle = 0°), the rough information of the relative molecular orientation developed during annealing treatment could be obtained.

Fig. 4 presents the intensity difference between EQ and ME scans of (110) peak as a function of annealing time. The difference of the peak intensity ($I_{(EQ)} - I_{(ME)}$) in both annealing temperatures tends to strongly increase with increasing annealing time in the first 60 min of annealing at both temperatures and after that tend to saturation. Thus, it could be implied that the relative level of molecular orientation of iPP

crystalline phase in the annealed iPP films is relatively increased with annealing time up to 60 min and then levels off. This result is similar to the trend of increase in true crystallinity (see Fig. 3a) and also is in good agreement with the previous works [47-50]. The increase in the relative level of molecular orientation of crystalline phase could mainly result in the significant improvement of mechanical properties of the materials, corresponding to the strong enhancement in Young's modulus and tensile strength of the annealed iPP films as presented in Figs. 9a and 9b, respectively.

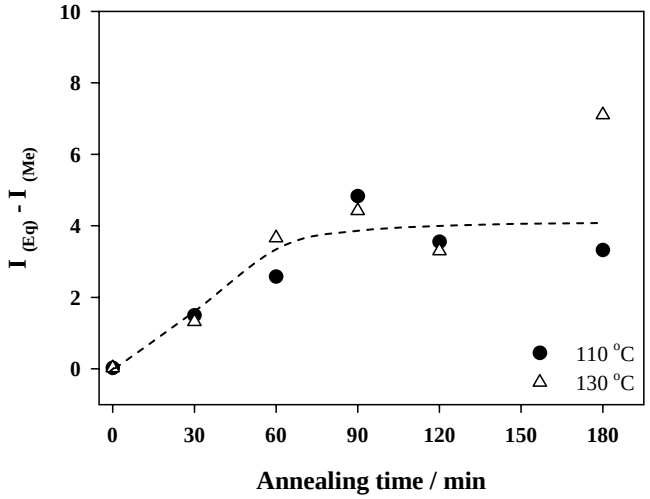

Fig. 4. Plot the intensity difference ($I_{(EQ)}$-$I_{(ME)}$) of (110) peak as a function of annealing times for the uniaxially drawn iPP thin films annealed at 110 and 130 °C.

Thermal Properties

The DSC curves for the uniaxially drawn iPP thin films annealing at 110 and 130 °C at different times are shown in Figs. 5a and 5b, respectively. All DSC curves clearly exhibit three prominent transition peaks defined as T_m^{sm}, T_c and T_m on increasing temperature, corresponding to a small endotherm, followed by a small exotherm and a sharp endotherm at around 161 °C, respectively. For the unannealed iPP film (UA), the first small endothermic peak (T_m^{sm}) is quite broader and is located in the temperature range of 45-85 °C with a maximum at about 70 °C. This peak reveals the presence of the smectic metastable phase of iPP and has been attributed to the melting of small monoclinic crystals developed on quenching process of the final product, reported by other research groups [2, 3, 5, 19]. In addition, the value of T_m^{sm} can also be taken as a simple indication of the order perfection of the material at different annealing conditions [3]. It is also seen that T_m^{sm} of the annealed samples shifts toward and increases with increasing annealing temperature and time, indicating that the order perfection of crystallinity increases with annealing temperature and time. As a result, the T_m^{sm} of annealed samples depends not only on the annealing temperature, but also on the annealing times. This result is strongly related to the increases in the X_c, and L of the annealed iPP thin films revealed by WAXD as shown in Figs. 3a and 3b, respectively [3, 38, 51, 52].

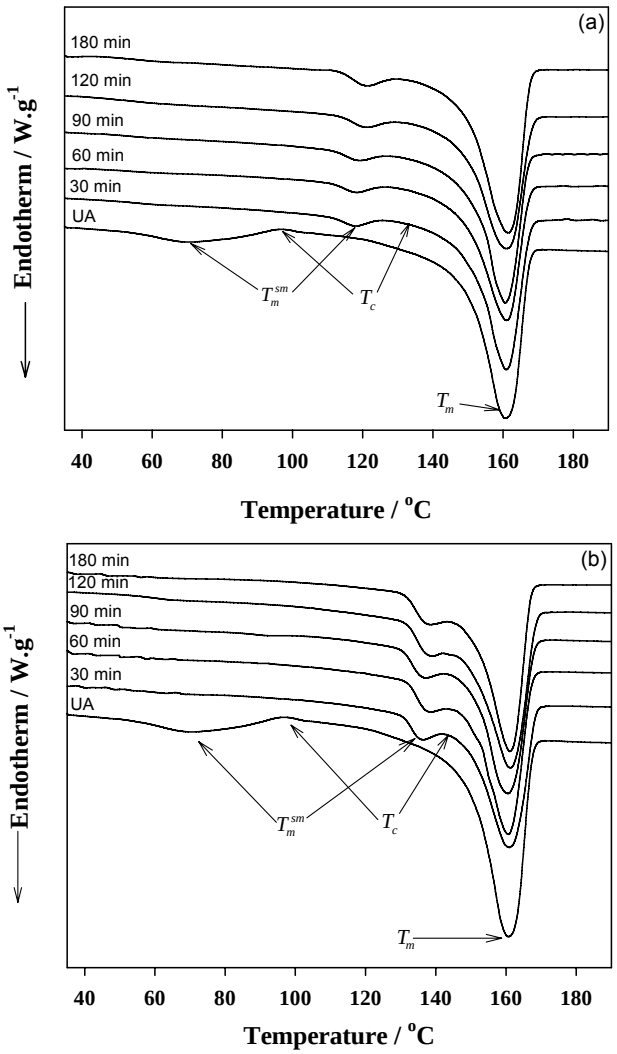

Fig. 5. DSC heating thermograms of the uniaxially drawn iPP thin films annealed at (a) 110 and (b) 130 °C at various times, measured at a heating rate of 10 °C /min.

Following the first endotherm, an exothermic transition peak (T_c) is present indicating that re-ordering process has occurred involving the recrystallization of the crystals just before melting in a more stable iPP form [3, 38]. In other words, this exothermic transition relates to the transformation of a paracrystalline/smectic phase to a monoclinic phase. The T_c of the UA iPP films is found in a broad range from 85-120 °C and centered at around 99 °C. While the T_c of the annealed iPP thin films is in a narrower range and increases with increasing annealing temperature and time (see Fig. 5), corresponding to the sharper and more intense WAXD patterns as shown in Figs. 1-2. Moreover, the apparent difference in the melting enthalpy area of the recrystallization peak (T_c) compared to the sharp melting peak (T_m) is obviously seen in all DSC curves. This result is in good agreement with the works of Ferrer-Balas *et al.* [3] and Alberola *et al.* [38], suggesting that the less stable microcrystallites progressively melt as the annealing temperature increase, whereas almost simultaneously, new crystallites which are increasingly thicker and more stable are formed (see Fig. 3), so that compensating the endothermic melting process by a re-ordering process involving energy dissipation. Nevertheless, the last main endothermic peaks (T_m) of the iPP films annealed at 110 and 130 °C at different

times are found to be unchanged and located at around 161 °C, indicating that it is independent of thermal history of the sample. In addition, this result suggests that thermal annealing does not significantly affect the stable monoclinic phase.

Fig. 6 represents the plot of apparent crystallinity obtained from DSC as a function of annealing times for the uniaxially drawn iPP thin films annealed at 110 and 130 °C. It is seen that the crystallinity significantly increases with annealing time and temperature. This is similar to the increase of true crystallinity (X_c) calculated from WAXD patterns (see Fig. 3). However, the values of crystallinity obtained by DSC measurement are quite smaller than that calculated from WAXD patterns. This could be due to the melting-recrystallization process of the sample until complete melting during heating scan.

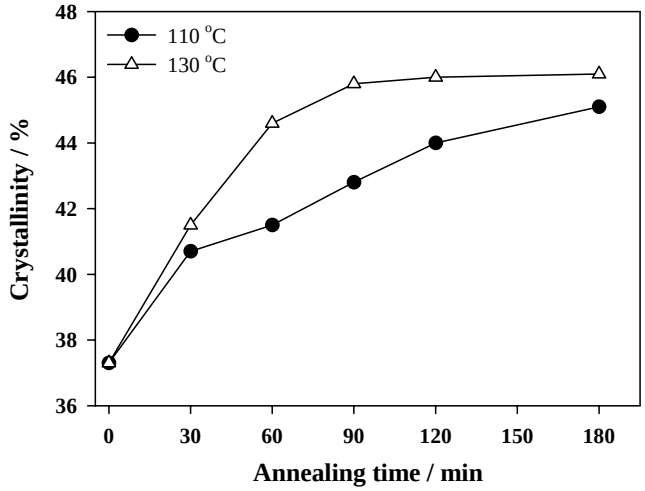

Fig. 6. The relationship between the apparent crystallinity and annealing time for the uniaxially drawn iPP thin film annealed at 110 and 130 °C.

Stress-strain behaviour

Figs. 7a and 7b present the example of the stress-strain curves of unannealed (UA) and drawn iPP thin films annealing at 110 °C at different times in both machine (MD) and transverse (TD) directions, respectively. It is seen that the profiles of stress-strain behavior of all annealed films in both MD and TD directions are similar to that of the UA iPP thin film. It exhibits the yield point followed with stress plateau and after that the strain hardening occurs. Clearly, the stress of all annealed iPP thin films is considerably higher than that of the UA film in each direction. Thus the yield stresses of all annealed iPP thin films are much higher than that of the UA film. The significant increase in yield stress of annealed films could be due to the higher degree of perfection of crystalline phase and the thickening of the crystal size as well as the reduction of both of the smectic and amorphous phases after isothermal annealing as confirmed by WAXD and DSC results shown in Figs. 1-6 [38, 51, 53]. In addition, the presence of the stress plateau could be attributed to the deformation of the PP smectic phase that still remained even when the films were annealed for a long period of time as supported by the WAXD and DSC results. The MD and TD stress-strain curves of the uniaxially drawn iPP thin films annealing at 130 °C are found to be of similar behaviour to that of iPP films annealing at 110 °C (picture not shown here).

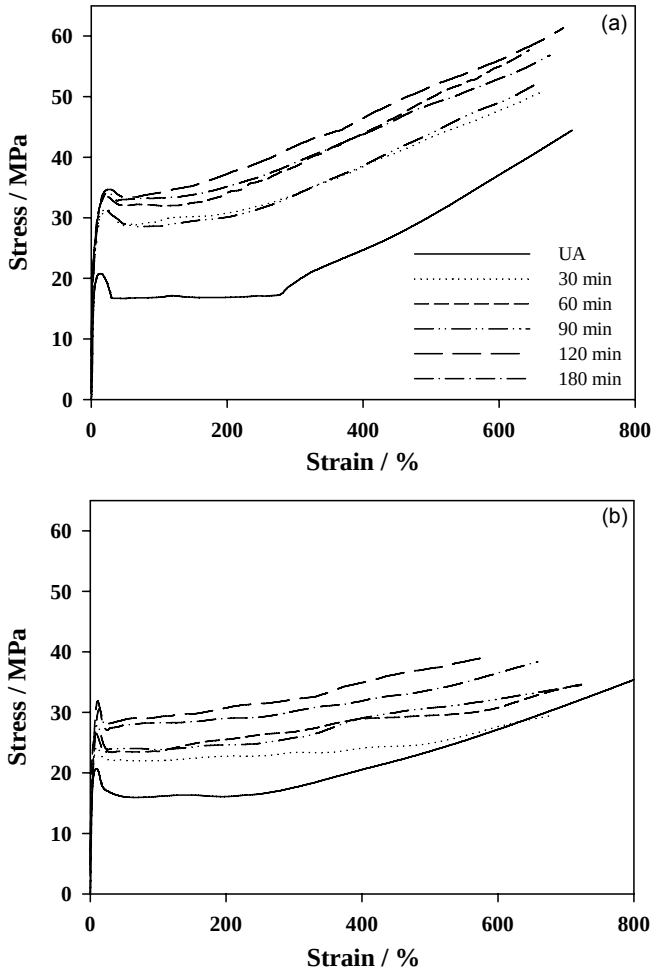

Fig. 7. Stress-strain curves of the uniaxially drawn iPP thin films annealed at 110 °C at various annealing times in (a) MD and (b) TD.

However, its MD stress plateaus are much shorter than those films annealing at 110 °C. This indicates that the portion of smectic phase in the films annealing at 130 °C is less than that of the films annealing at 110 °C, corresponding to the increase in degree of crystallinity obtained from the WAXD and DSC experiments (see Figs. 3 and 6). Also, the stress values in MD and TD directions of the film annealed at 130 °C are somewhat higher than those of the film annealing at 110 °C. As a result, the higher mechanical properties of the film annealing at 130 °C than those of the film annealing at 110 °C could be observed as shown in Fig. 8.

Mechanical properties

The Young's modulus, tensile strength and elongation at break in both MD and TD directions as a function of annealing times are displayed in Figs. 8a-c, respectively, for the drawn iPP films annealing at both 110 and 130 °C. As shown in Fig. 8a, the MD and TD Young's moduli of both annealed iPP films strongly enhance with increasing annealing times up to 60 min and after that tend to level off, corresponding to an increase in true crystallinity (X_c), apparent crystal size (L) and the relative level of molecular orientation as presented in Figs. 3 and 4. The Young's moduli of iPP thin films annealed at 130 °C are significantly higher than those of films annealing at

110 °C in both directions. This could be due to the higher crystallinity, more degree of perfection of crystallites and more thickening crystal size obtained from the higher thermodynamic mobility of the iPP chain segments as annealing at the higher temperature (see Figs. 3 and 6) [1-3,38-41].

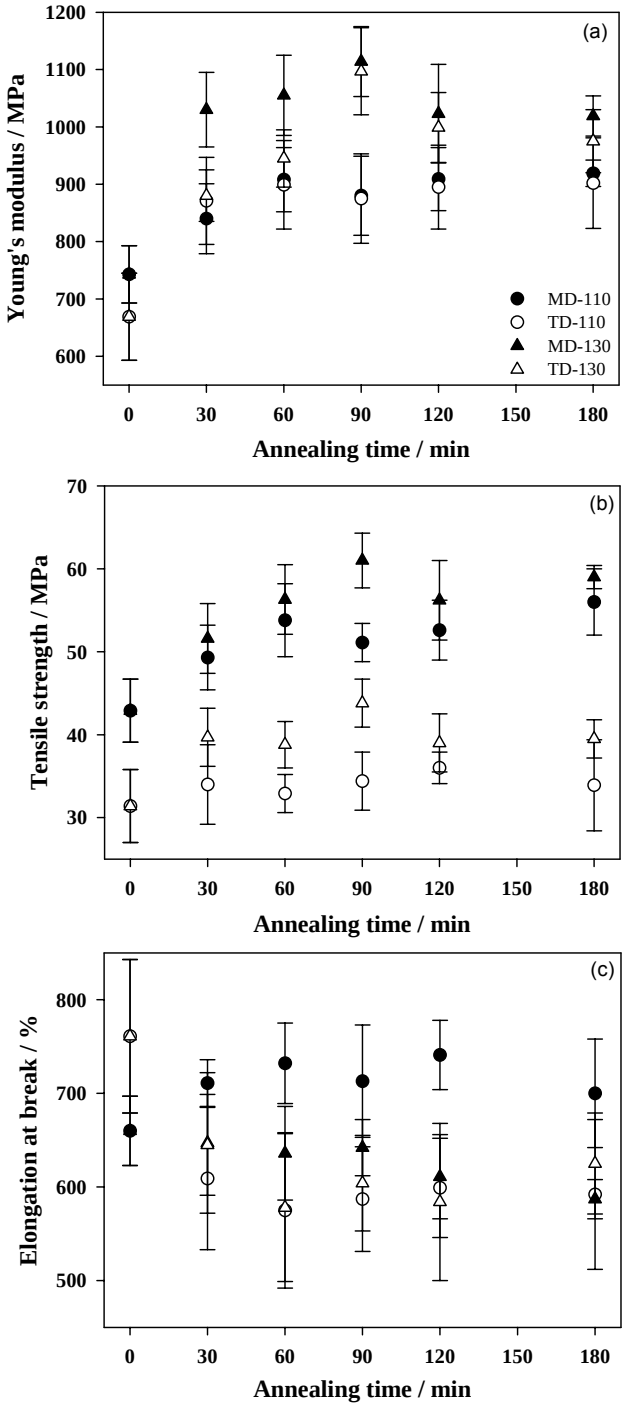

Fig. 8. Mechanical properties in MD and TD directions of the uniaxially drawn iPP thin films annealed at 110 and 130 °C at different annealing times: (a) Young's modulus, (b) tensile strength and (c) elongation at break.

Interestingly, the values of Young's modulus of all annealed iPP films at 110 °C in both MD and TD directions are very slightly different, indicating that the sample exhibits almost isotropic property, though the UA film was of slightly higher anisotropy. The possible reasons could be due to; a) the highly improved crystalline portions in TD direction which is close to the same level in the MD direction after annealing (see Fig. 3a) because there is much more free volume for easily molecular motion ability of amorphous phase to be packed and b) the more van der Waals inter-chain forces owing to the closed packed crystal regions developed highly in TD direction after annealing. Nevertheless, the variation in modulus of all annealed films is seen. This could be mainly affected by the variation of molecular orientation of the crystalline portion as shown in Fig. 4.

Comparison of the MD and TD moduli of the annealed films with that of the UA film reveals that the MD and TD moduli of the films annealing at 110 °C for 60 min are higher by about 22 % and 34 %, respectively, while the MD and TD moduli of films annealing at 130 °C for 60 min are higher by about 42 % and 41 %, respectively. Thus, the MD Young's modulus of the films annealing at 130 °C is about two times higher than that of the film annealing at 110 °C, corresponding to the higher improvement of crystallinity and crystal thickness of film annealing at 130 °C (see Figs. 3 and 6). These results match well with the fact that the crystallinity, crystal size, perfection of crystal and molecular orientation of annealed iPP films are strongly higher than that of the UA film, as reported in WAXD and DSC results [1-3, 21, 51, 53, 54].

From Fig. 8b, it is seen that the MD and TD tensile strengths of all annealed films tend to drastically increase with increasing annealing times up to 60 min and after that tends to level off, especially in the films annealing at 130 °C. On comparison of the MD tensile strength of annealed iPP thin films to that of UA film, the increase in MD tensile strengths of films annealing at 110 and 130 °C at 60 min are about 25 % and 31 %, respectively. While TD tensile strength of the film annealed at 110 and 130 °C at 30 min are about 5 % and 26 %, respectively. These results could be due to the more perfection of crystalline phases, the thicker crystal size and the higher relative level of molecular orientation as well as the stronger interactions of iPP inter-chain segments after rearrangement of their registrations which are developed in the films annealed at 130 °C, as confirmed by the WAXD and DSC results (see Figs. 1-6) [1-3, 19-21, 51, 53]. However, TD tensile strength is 5 times lower than MD tensile strength for the film annealed at 110 °C; this could be attributed to the decrease in the physical cross-linking degree of the amorphous phase even when the size of the crystalline entities is increased. Thus, it could be proposed that the tensile strength of iPP film is governed not only by the degree of crystallinity but also by the degree of physical cross-linking degree of the amorphous phase induced by the crystalline phase [51].

From Fig. 8c, it is seen that almost MD and TD elongation at breaks of both annealed films are slightly decreased, indicating that the ductility of the annealed iPP films was reduced. The drop in MD elongation at break of the films annealed at 130 °C compared to that of the unannealed one is about 10 %, whereas the drop in TD elongation at break of the both annealed films is in the same range of ~ 20%. The reduction in elongation at break of the annealed iPP films could be viewed as a result of the reduction of molecular mobility [19, 55], the decrease in the portion of smectic and amorphous phases (see Figs. 1-2) and the increase in the degree of perfection

of crystallites (see Figs. 3 and 6) and the increase in physical cross-linking degree of amorphous phase [51].

Generally, the properties of polymer samples depend on the fabrication techniques/processing conditions. Therefore, we cannot directly compare the properties of polymers prepared by different conditions/techniques. Thus we cannot directly compare this work to other research works. However, the qualitative comparison of iPP's properties in this work to those of iPP samples which were prepared by different techniques and were annealed at the different temperatures might be drawn. The mechanical properties, crystallinity and apparent crystal size of the iPP thin films in this work were found to be lower than those of the annealed iPP samples reported by Ferrer-Balas *et al.* [3], especially at the higher annealing temperature (>130 °C). Moreover, with the results obtained from the present work, Ferrer-Balas [3], Alberola [22,33] and Natale [21], it could be suggested that the modulus, crystallinity and apparent crystal size of annealed iPP samples will be enhanced with increasing annealing temperature but the ductility of samples would be inversely decreased.

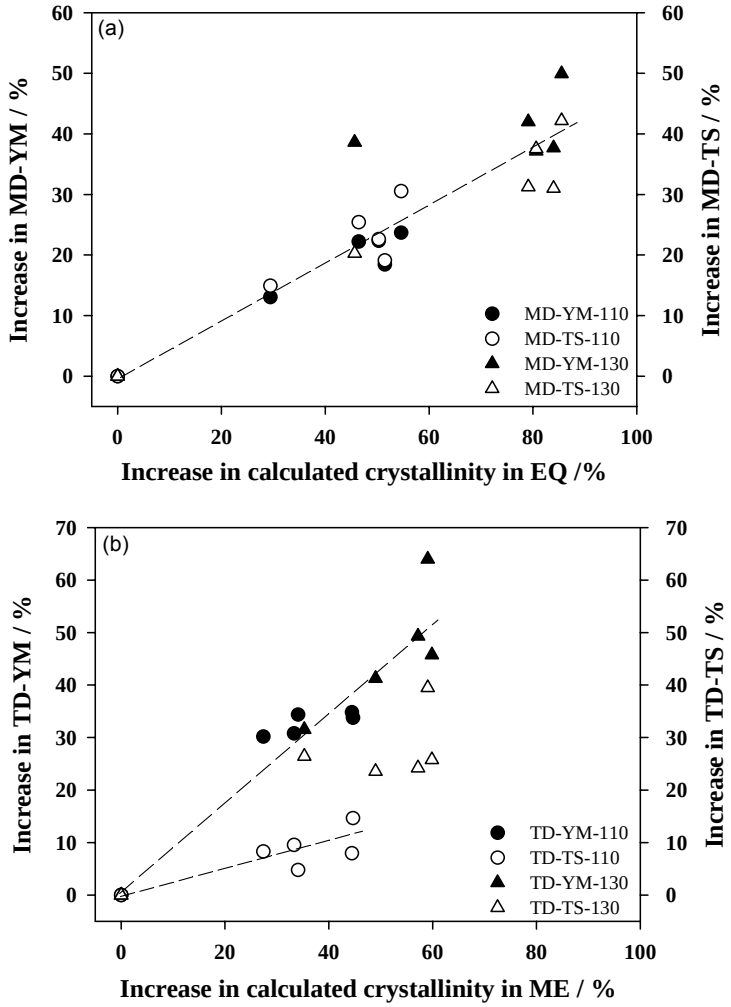

Fig. 9. Correlation of increase in Young's modulus (YM) and tensile strength (TS) with increase in true crystallinity (X_c) in both (a) MD and (b) TD directions for the uniaxially drawn iPP thin films annealed at 110 and 130 °C.

Correlation between mechanical and microstructural properties

The correlation between mechanical properties and the true and apparent crystallinities of the uniaxially drawn iPP thin films annealed at 110 and 130 °C at different annealing times is now examined. In this section, the increase in modulus and strength of annealed film is supposed to correlate with the increase in crystallinity. Thus the plots of increase in Young's modulus (YM) and tensile strength (TS) in both MD and TD directions against the increase in true crystallinity (calculated from WAXD patterns) and apparent crystallinity (measured by DSC) for the annealed drawn iPP films were established in order to observe their correlations and evaluate the suitable parameters. The plots of increase in YM and TS in the both MD (MD-YM and MD-TS) and TD directions (TD-YM and TD-TS) versus the increase in true crystallinity in equatorial (EQ) and meridian (ME) sections are presented in Figs. 9a and 9b, respectively, for the iPP films annealed at 110 and 130 °C. From Fig. 9a, the increase in MD-YM and MD-TS shows a good trend of linear correlation with an increase in true crystallinity in EQ in both annealing temperatures.

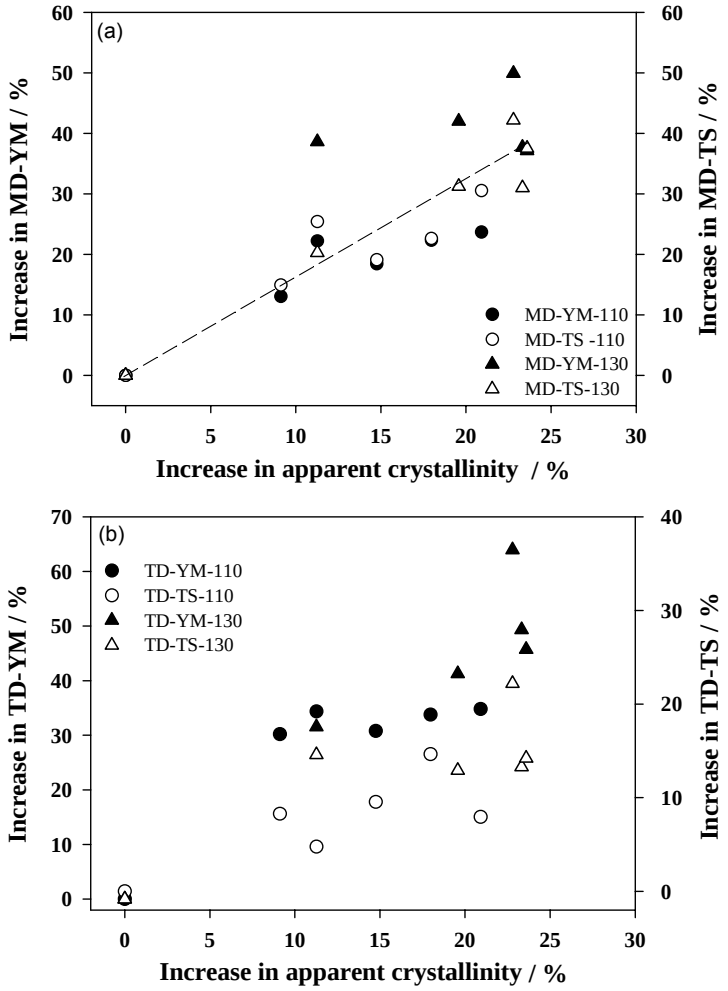

Fig. 10. Correlation of increase in Young's modulus (YM) and tensile strength (TS) with increase in apparent crystallinity in both (a) MD and (b) TD directions for the uniaxially drawn iPP thin films annealed at 110 and 130 °C.

Also, some linear relationships are found between the increases in TD-YM and TD-TS with an increase in true crystallinity in ME in both annealing temperatures (see Fig. 9b). This could be suggested that the true crystallinity well corresponds to the increase in both of YM and TS in both MD and TD directions of the annealed iPP films which is similar to the work of Ferrer-Balas *et al.* [3].

Also, the correlations of increase in MD-YM, MD-TS and TD-YM, TD-TS with increase in the apparent crystallinity are plotted in Figs. 10a and 10b for MD and TD directions, respectively. It can be observed from Fig. 10a that the increase in MD-YM and MD-TS exhibits less linear relationship with an increase in apparent crystallinity and the data points show highly fluctuation from the linearity trend. Moreover, no linear correlation of increase in TD-YM and TD-TS with increase in the apparent crystallinity could be found (see Fig. 10b). Therefore, from the correlation plots shown in Figs. 9 and 10, the true crystallinity calculated from X-ray patterns in each EQ and ME scans is found to be a more suitable parameter to correlate with the increase in YM and TS in both MD and TD directions than the apparent crystallinity obtained from DSC measurement.

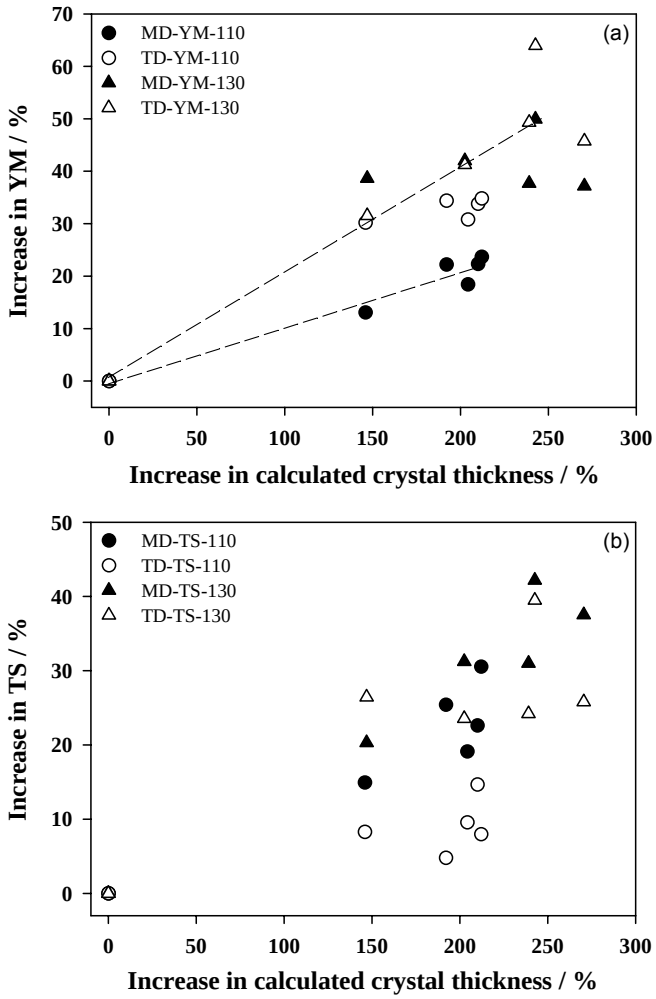

Fig. 11. The relationship between (a) Young's modulus and (b) tensile strength and the apparent crystal thickness in both MD and TD directions.

In addition, the relationship between the increase in YM and TS in both MD and TD directions and the increase in apparent crystal size (*L*) is also studied as plotted in Fig. 11. Some linear relationships of increase in YM in both MD and TD direction with increase in crystal thickness for both annealing temperatures can be observed. The slope of linearity of TD-YM and crystal thickness of samples annealed at 110 °C is seen to be steeper than that of MD-YM. However, the slopes of linearity of YM with crystal thickness in both MD and TD directions for the samples annealed at 130 °C appeared to be equal and steeper than those of sample annealed at 110 °C. Thus from this result it could be suggested that the increase in crystal thickness exhibits a stronger effect on increase in TD-YM rather than in MD-YM, in particular for the film samples annealed at 110 °C. However, for the relationship between increase in TS and increase in crystal thickness in both MD and TD directions, it can not observe any relation as shown in Fig. 11b, suggesting that the crystal thickness is not a suitable parameter to use to relate the increase in TS of the annealed film.

Conclusions

The effect of annealing on the microstructure, molecular orientation, thermal and mechanical properties of uniaxially drawn iPP thin film was investigated using WAXD, DSC and tensile testing, respectively. Under the studied annealing conditions (at 110 and 130 °C), the smectic phase was transformed gradually to the more stable phase with increasing annealing temperature and time, as seen from WAXD and DSC results. The estimated level of molecular orientation of annealed films was also increased with annealing time and could be directly affected by the variation of mechanical properties. The degree of true and apparent crystallinities was strongly increased with increasing annealing temperature and time, especially at the higher annealing temperature. The T_m^{sm} of the annealed film is found to increase with annealing time and temperature indicating the higher degree of perfection of material. It is also found that the true crystallinity is a more suitable parameter to correlate with the increase in Young's modulus (YM) and tensile strength (TS) in both machine (MD) and transverse (TD) directions than the apparent crystallinity. In addition, the crystal thickness of the annealed iPP films seems to well relate to only Young's modulus not to tensile strength and tends to exhibit a greater effect on the increase in TD-YM rather than in MD-YM. Therefore, the transformation of smectic phase to monoclinic phase, the more degree of perfection of crystallite, the more lamellar thickening, the increase in crystallinity and the enhancement of molecular orientation could be the important factors for the significant improvement of mechanical properties of the uniaxially drawn iPP thin films treated under the appropriate annealing conditions.

Experimental part

Materials and Thin Film Preparation

A commercial isotactic polypropylene (iPP), trade name PRO-FAX 6631, with melt flow index of 2 g/10 min and a density of 0.903 g/cm^3 was kindly supplied by HMC Co., Thailand. The iPP pellets were fabricated as an extruded film using a mini-extruder (Randcastle RCP-0625) equipped with a cast film line. The screw speed was 70 rpm and the temperature profile was 245/280/290/295 °C, represented for the hopper zone, two barrel zones and slit die zone, respectively. The gap at the die lip and the width were fixed at 0.065 and 15.2 cm, respectively. The film exiting from the

die outlet was immediately cooled on the chilled roll and was rapidly uniaxial drawn to obtain film draw ratio of about 30 (a die gap to film thickness ratio). Thus, the film thickness about 20 μm was obtained and used throughout this work.

Annealing Procedure

According to our previous work [48], smectic phase in the drawn iPP and thermotropic liquid crystalline polymer/PP *in-situ* composite films was observed to transform to a more stable phase (i.e. α-form) after the films were annealed at 110 °C for 2 h. Therefore, in order to investigate the effect of annealing temperature and time on the properties of drawn iPP thin film in more detail, the films were annealed in an air oven at two fixed low-temperature ranges, i.e. 110 and 130 °C, assigned following Drozdov *et al.* [45], at various times from 30 to 180 minutes. Moreover, annealed iPP thin film with a smooth surface cannot be prepared for the annealing temperature ≥ 140 °C. The accuracy of the oven temperature was ± 2 °C. When the required annealing time was reached, the samples were quickly removed from the oven and quenched in air at room temperature in order to freeze the developed structural rearrangement. These specimens were then stored at ambient temperature for at least 24 h before further analysis.

Wide angle X-ray diffraction (WAXD)

To determine the microstructural transformation, the true crystallinity, and apparent crystal sizes of the samples, WAXD experiments were performed. In order to archive the appropriate X-ray diffraction intensity, a thick film (~0.9 mm) was prepared by folding several layers of the thin film, while maintaining its relative MD direction. The WAXD measurement was performed at room temperature, using Ni-filtered Cu-K_α radiation of wavelength 0.154178 nm, on a Philips X-ray diffractometer (X' Pert MPD) operating at 40 kV and 35 mA. The scan range was varied from 5 to 50° in steps of $\Delta 2\theta$ = 0.2° with a count time of 5 s at each position. The WAXD intensity profiles were measured in both equatorial (EQ) and meridional (ME) sections. The X-ray intensity of each sample was normalized by the peak intensity at 43.0° which have equal intensity in both sections. From the WAXD patterns the degree of crystallinity (X_c), true crystallinity, of the annealing samples was calculated in both sections by assuming the contribution of the crystalline and amorphous portions to the area of diffraction patterns [56]. Also, the crystal thickness (L) was deduced using the Scherrer equation [3]:

$$L = 0.9\lambda / \left(\frac{D\pi}{180} \right) \cos\theta$$

where L is the apparent crystal size (Å), λ is the wavelength used (Å), D is the half-height angular width (degree), and θ is the position of the maximum diffraction.

Differential scanning calorimetry (DSC)

To investigate the thermal behaviours and evaluate the apparent crystallinity of the drawn iPP films influenced by heat treatments, the annealed samples were analysed using DSC, METTLER TOLEDO 823^e. Pure standard indium was used as a reference material to calibrate the temperature and the heat flow. The drawn iPP film sample cut into small pieces weighed about 5 mg was crimped in aluminium pans. The scans were performed under nitrogen atmosphere from 30 to 200 °C at a

scanning rate of 10 °C/min. The melting temperatures of smectic and monoclinic phases, T_m^{sm} and T_m, respectively, were reported from the peak temperatures of the endotherms. The recrystallization temperature (T_c) was also presented. The crystallinity was determined from the measured heat of fusion, assuming that an average value for the heat of fusion of 100% crystalline PP equals to 207.1 J/g [57].

Mechanical properties

The unannealed (UA) and annealed iPP films were tested at room temperature using a Lloyds tensile testing machine (LR series) with a gauge length of 2.50 cm, a crosshead speed of 5.00 cm/min and a full-scale load cell of 0.5 kN. All films prepared at the draw ratio ~30 were cut into a dumbbell-shape (size = 2.50 × 4.00 cm^2) by using a punching machine. An average value of at least 10 measurements in each sample was determined in both MD and TD. All data were collected and analysed using a package program "LR series".

Acknowledgements

This work was financially supported by the Thailand Research Fund and the Higher Commission Committee (Grant no. MRG4780032). Mahidol University and Polymer Science Centre, University of Reading, UK, are fully acknowledged for providing their facilities and support. The author would also like to thank Prof. Sauvarop Bualek-Limcharoen and Dr. Supaporn Sangribsub for their helpful discussions.

References

[1] O´Kane, W.J.; Young, R.J.; Ryan, A.J. *J. Macromol. Sci.-Phys.* **1997**, *B34*, 427.
[2] Poussin, L.; Bertin, Y.A.; Parisot, J.; Brassy, C. *Polymer.* **1998**, *39(18)*, 4261.
[3] Ferrer-Balas, D.; Maspoch, M.L.; Martinez, A.B.; Santana, O.O. *Polymer.* **2001**, *42(4)*, 1697.
[4] Aboulfaraj, M.; G´Sell, C.; Ulrich, B.; Dahoun, A.; *Polymer*. **1995**, *36*, 731.
[5] Seguela, R.; Staniek, E.; Escaig, B.; Fillon, B. *J. App. Polym. Sci.* **1999**, *71*, 1873.
[6] Kiss, G. *Polym. Eng. Sci.* **1987**, *27(6)*, 410.
[7] Varga, J. *Polypropylene: Structure, blends and composites*, Vol.1, Ed.: Karger-Kocsis, J. **1995**, Chapman and Hall, London.
[8] Pötschke, P.; Kretzschmar, B.; Janke, A. *Comp. Sci. Tech.* **2007**, *67(5)*, 855.
[9] Bao, S.P.; Tjong, SC. *Mat. Sci. Eng. A.* **2008**, *485*, 508.
[10] Natta, G. *SPE J.* **1959**,*15*, 373.
[11] Turner-Jones, A.; Atzelewood, J.M.; Beckett, D.R. *Makromol. Chem. Basel*. **1964,** *75*, 134.
[12] Bruckner, S.; Meille, S.V.; Petraccone, V.; Pirozzi, B. *Prog. Polym. Sci.* **1991,** *16*, 361.
[13] Meille, S.V.; Ferro, D.R.; Brueckner, S.; Lovinger, A.J.; Padden, F.J. *Macromolecules* **1994,** *27*, 2615.
[14] Tjong, S.C.; Shen, J.S.; Li, R.K.Y.S.; *Polymer* **1996,** *38*, 2309.
[15] Karger-Kocsis, J.; Varga, J.; Ehrenstin, G.W. *J. Appl. Polym. Sci.* **1997**, *64*, 2057.
[16] Sauer, J.A.; Pae, K.D. *J. Appl. Phys.* **1968**, *39*, 4959.
[17] Campbell, R.A.; Phillips, P.J. *Polymer* **1993**, *34*, 4809.
[18] Mark, J.E. *Physical properties of polymers handbook*. **1996**, AIP press, New York.

[19] O'Kane, W.J.; Young, R.J.; Ryan, J.; Bras, W.; Derbyshire, G.E.; Mant, G.R. *Polymer*, **1994**, *35*, 1352.
[20] Wang, Z-G.; Hsiao, B.S.; Srinivas, S.; Brown, G.M.; Tsou, A.H.; Cheng, Z.D.; Stein, R.S. *Polymer*, **2001**, *42(18)*, 7561.
[21] Natale, R.; Russo, R.; Vittoria, V. *J. Mat. Sci.* **1992**, *27*, 4350.
[22] Miller, R.L. *Polymer*, **1960**, *1(2)*, 135.
[23] Ferrerp, A.; Ferracini, E.; Massavillani, A.; Malta, V. *J. Macromol. Sci. Phys.* **2000**, *B39*, 109.
[24] Grebowicz, J.; Lau, J.F.; Wunderlich, B. *J. Polym. Sci. Polym. Symp.* **1984,** *71*, 19.
[25] Natta, G.; Peraldo, M.; Corradini, P. *Rand. Accad. Naz. Lincei*. **1959**, *26*, 14.
[26] Natta, G.; Corradini, P. *Suppl. Nuovo. Cimento. Suppl.* **1960**, *15*, 40.
[27] Hsu, C.C.; Geil, P.H.; Miyaji, H.; Asai, K. *J. Polym. Sci. Phys.* **1986**, *24*, 2379.
[28] Wyckoff, H.W. *J. Polym. Sci.* **1962**, *62(173),* 83.
[29] Morosoff, N.; Peterlin, A. *J. Polym. Sci. Polym. Phys.* **1972**, *10*, 1237.
[30] Zuo, F.; Keum, J.K.; Chen, X.; Hsiao, B.S.; Chen, H.; Lai, S-Y.; Wevers, R.; Li, J. *Polymer* , **2007**, *48*, 6867.
[31] McAllister, P.B.; Carter, T.J.; Hinde, R.M. *J. Polym. Sci. Phys.* **1978**, *16*, 49.
[32] Bodor, G.; Grell, M.; Kallo, A. *Faserforsch. TextilTech* .**1964,***15* , 527.
[33] Caldas, G.; Brown, G.R.; Nohr, R.S.; MacDonald, J.G.; Raboin, L.E. *Polymer* **1994,** *35*, 899.
[34] Ferrero, A.; Ferracini, E.; Mazzavillani, A.; Malta, V. *J. Macromol. Sci. Phys. **2000**, B39,* 109.
[35] Saraf, R.; Portor, R.S. *Molec. Cryst. Liq. Cryst. Lett.* **1985**, *2*, 85.
[36] Vittoria, V. *J. Macromol. Sci. Phys.* **1989,** *B28*, 489.
[37] Zanetti, R.; Celotti, G.; Fichera, A.; Francesconi, R. *Makromol. Chem.* **1969**, *128, 137.*
[38] Alberola, N.; Fugier, M.; Petit, D.; Fillon, B. *J. Mat. Sci.* **1995**, *30*, 1187.
[39] Jia, J.; Raabe, D. *Eur. Polym. J.* **2006**, *42*, 1755.
[40] Frontini, P.M.; Fave, A. *J. Mat. Sci.* **1995**, *30*, 2446.
[41] Greco, R.; Ragosta, G. *J. Mat. Sci.* **1988**, *23*, 4171.
[42] Wunderlich, B. *Macromolecular physics*, vol. 2. **1976,** New York, Academic.
[43] Xu, T.; Yu, J.; Jin, Z. *Mat. Des.* **2001**, *22*, 27.
[44] Pegoretti, A.; Kolarik, J.; Fambri, L.; Penati, A. *Polymer* **2003**, *44*, 3381.
[45] Drozdov, A.D.; Christiansen, J.C. *Eur. Polym. J.* **2003**, *39(1)*, 21.
[46] Zia, Q.; Androsch, R.; Radusch, H-J.; Piccarolo, S. *Polymer* **2006**, *47(24)*, 8163.
[47] Song, Y.; Nemoto, N. *Polymer* **2006**, *47(1)*, 489.
[48] Saengsuwan, S.; Mitchell, G.R.; Bualek-Limcharoen, S. *Polymer* **2003**, *44*, 5951.
[49] Minardi, A.; Boudeulle, M.; Duval, E.; Etienne, S. *Polymer* **1997**, *38*, 3957.
[50] Aoyagi, Y.; Doi, Y.; Iwata, T. *Polym. Deg. Stab.* **2003**, *79*, 209.
[51] Alberola, N.; Fugier, M. ; Petit, D. ; Fillon, B. *J. Mat. Sci.* **1995**, *30*, 860.
[52] Jourdan, C.; Cavaille, J.Y.; Perez, J. *J. Polym. Sci. Polym. Phys.* **1980**,*18*, 493.
[53] Vittoria, V.; Perullo, A. *J. Macromol. Sci. Phys.* **1986**, *B25(3)*, 267.
[54] Rolando, R.J.; Krueger, W.L.; Morris, H.W. *Polym. Mater. Sci. Eng*. **1985**, *52*, 76.
[55] Chu, P.P.J.; Huang, W.J.; Chang, F.C. *Polymer* **2000**, *42*, 2185.
[56] Young, R.J.; Lovell, P.A*. Introduction to polymers* (2 ed.), **1991**, Chapman and Hall, London.
[57] Mettler Toledo. Thermal Analysis UserCom **1995**; *1*.